Intravoxel Incoherent Motion–derived Histogram Metrics for Assessment of Response after Combined Chemotherapy and Radiation Therapy in Rectal Cancer: Initial Experience and Comparison between Single-Section and Volumetric Analyses[1]

Stephanie Nougaret, MD, PhD
Hebert Alberto Vargas, MD
Yulia Lakhman, MD
Romain Sudre
Richard K. G. Do, MD, PhD
Frederic Bibeau, MD, PhD
David Azria, MD, PhD
Eric Assenat, MD, PhD
Nicolas Molinari, PhD
Marie-Ange Pierredon, MD
Philippe Rouanet, MD, PhD
Boris Guiu, MD, PhD

Purpose: To determine the diagnostic performance of intravoxel incoherent motion (IVIM) parameters and apparent diffusion coefficient (ADC) to assess response to combined chemotherapy and radiation therapy (CRT) in patients with rectal cancer by using histogram analysis derived from whole-tumor volumes and single-section regions of interest (ROIs).

Materials and Methods: The institutional review board approved this retrospective study of 31 patients with rectal cancer who underwent magnetic resonance (MR) imaging before and after CRT, including diffusion-weighted imaging with 34 *b* values prior to surgery. Patient consent was not required. ADC, perfusion-related diffusion fraction *(f)*, slow diffusion coefficient *(D)*, and fast diffusion coefficient *(D*)* were calculated on MR images acquired before and after CRT by using biexponential fitting. ADC and IVIM histogram metrics and median values were obtained by using whole-tumor volume and single-section ROI analyses. All ADC and IVIM parameters obtained before and after CRT were compared with histopathologic findings by using *t* tests with Holm-Sidak correction. Receiver operating characteristic curves were generated to evaluate the diagnostic performance of IVIM parameters derived from whole-tumor volume and single-section ROIs for prediction of histopathologic response.

Results: Extreme values aside, results of histogram analysis of ADC and IVIM were equivalent to median values for tumor response assessment ($P > .06$). Prior to CRT, none of the median ADC and IVIM diffusion metrics correlated with subsequent tumor response ($P > .36$). Median *D* and ADC values derived from either whole-volume or single-section analysis increased significantly after CRT ($P \leq .01$) and were significantly higher in good versus poor responders ($P \leq .02$). Median IVIM *f* and *D** values did not significantly change after CRT and were not associated with tumor response to CRT ($P > .36$). Interobserver agreement was excellent for whole-tumor volume analysis (range, 0.91–0.95) but was only moderate for single-section ROI analysis (range, 0.50–0.63).

Conclusion: Median *D* and ADC values obtained after CRT were useful for discrimination between good and poor responders. Histogram metrics did not add to the median values for assessment of tumor response. Volumetric analysis demonstrated better interobserver reproducibility when compared with single-section ROI analysis.

Online supplemental material is available for this article.

[1] From the Department of Abdominal Imaging, Saint Eloi University Hospital, CHU Montpellier, 80 Avenue Augustin Fliche, 34295 Montpellier Cedex 5, France (S.N., M.A.P., B.G.); Institute of Cancer Research of Montpellier (IRCM-U1194), Montpellier, France (S.N., F.B., D.A., B.G.); INSERM, Unit 896, Montpellier, France (S.N., B.G.); Department of Radiology, Memorial Sloan Kettering Cancer Center, New York, NY (H.A.V., Y.L., R.K.G.D.); Departments of Radiology (R.S.), Histopathology (F.B.), Oncology and Radiation Therapy (D.A., E.A.), and Surgery (P.R.), Montpellier Cancer Institute, Montpellier, France; and Department of Statistics–IMAG, Montpellier University, CHU Montpellier, Montpellier, France (N.M.). Received March 24, 2015; revision requested May 4; revision received October 26; accepted November 30; final version accepted January 8, 2016. Supported by INCa, SIRIC Montpellier, and French Society of Radiology (S.N.). **Address correspondence to** S.N. (e-mail: *stephanienougaret@free.fr*).

Changes in the treatment of patients with locally advanced rectal cancer highlight the need for accurate assessment of tumor response to combined chemotherapy and radiation therapy (CRT). In the past, CRT was followed by surgical resection in nearly all patients, irrespective of response to CRT (1–4). However, new data suggest that surgery may not be necessary in patients with complete response (5–8). Several imaging modalities allow noninvasive evaluation of morphologic and functional changes in tumors after CRT. Fluorine 18 fluorodeoxyglucose positron emission tomography (9,10) and conventional T1- and T2-weighted magnetic resonance (MR) imaging have been extensively studied for this purpose (11–13). However, diagnostic assessment by using either of these techniques is hampered by difficulties in differentiating residual tumor from radiation-induced fibrosis (14). In other studies, investigators have suggested that adding diffusion-weighted imaging (DWI) to conventional MR imaging can aid in this differentiation and thus improve the prediction of response after neoadjuvant therapy (15–23). However, the literature on use of the apparent diffusion coefficient (ADC) for assessment of rectal tumor response to CRT is inconsistent. While some authors found lower pre-CRT ADC values in good responders compared with poor responders (15), others reported no difference (24). Several studies have demonstrated significantly higher mean posttreatment ADC values in complete responders compared with patients with residual disease (17,22,24), whereas others reported no difference (19). These conflicting conclusions may be attributed to several factors, including technical differences between DWI sequences used in each study (eg, the use of different *b* values and failure to distinguish perfusion effects from true tissue diffusion when using monoexponential fitting of the DWI signal across *b* values) and inability to capture tumor heterogeneity when calculating mean or minimum diffusion parameters obtained from single-section regions of interest (ROIs). We hypothesize that issues related to the technical aspects of DWI could be overcome by using sufficient *b* value sampling and a biexponential curve fit analysis with the intravoxel incoherent motion (IVIM) model, while issues related to tumor heterogeneity could be addressed by means of histogram analysis of the entire tumor volume. Thus, the purpose of our study was to determine the diagnostic performance of IVIM parameters and ADC to assess response to CRT in patients with rectal cancer by using histogram analysis derived from whole-tumor volumes and single-section ROIs.

Advances in Knowledge

- Extreme values aside, histogram analysis findings of apparent diffusion coefficient (ADC) and intravoxel incoherent motion (IVIM) metrics were equivalent to median values for the assessment of tumor response to combined chemotherapy and radiation therapy (CRT) ($P > .06$).
- There was no association between median ADC or IVIM values prior to CRT and the subsequent tumor response to CRT ($P > .36$).
- Median slow diffusion coefficient *(D)* and ADC values increased significantly after CRT ($P \leq .01$) and were significantly higher in good responders to CRT versus poor responders ($P \leq .02$).
- Median perfusion-related diffusion fraction and fast diffusion coefficient values did not significantly change after CRT and were not associated with the degree of tumor response to CRT ($P > .36$).
- Median whole-tumor volume analysis of diffusion metrics had more robust interobserver agreement (range, 0.91–0.95) when compared with median single-section region of interest (ROI) analysis (range, 0.50–0.63).

Implication for Patient Care

- IVIM parameter *D* may be useful for assessment of tumor response to CRT in rectal cancer; whole-tumor volume is preferred over single-section ROI analysis because of its superior interobserver agreement and the potential to better capture the intratumoral heterogeneity.

Materials and Methods

Our institutional review board approved this retrospective study and waived the requirement for written informed consent. A search of the pathology database in the electronic medical records system at our institution yielded 123 patients

Published online before print
10.1148/radiol.2016150702 **Content codes:** GI MR

Radiology 2016; 280:446–454

Abbreviations:
ADC = apparent diffusion coefficient
AUC = area under the ROC curve
CRT = combined chemotherapy and radiation therapy
D = slow diffusion coefficient
DWI = diffusion-weighted imaging
*D** = fast diffusion coefficient
f = perfusion-related diffusion fraction
IVIM = intravoxel incoherent motion
ROC = receiver operating characteristic
ROI = region of interest

Author contributions:
Guarantors of integrity of entire study, S.N., Y.L., R.S., M.A.P., P.R., B.G.; study concepts/study design or data acquisition or data analysis/interpretation, all authors; manuscript drafting or manuscript revision for important intellectual content, all authors; approval of final version of submitted manuscript, all authors; agrees to ensure any questions related to the work are appropriately resolved, all authors; literature research, S.N., H.A.V., Y.L., R.S., M.A.P., P.R., B.G.; clinical studies, S.N., H.A.V., R.S., F.B., D.A., E.A., M.A.P., P.R., B.G.; experimental studies, S.N., R.S., M.A.P., P.R.; statistical analysis, S.N., R.S., N.M., M.A.P.; and manuscript editing, S.N., H.A.V., Y.L., R.S., R.K.G.D., D.A., M.A.P., P.R., B.G.

Funding:
This research was supported by the National Institutes of Health and National Cancer Institute Memorial Sloan Kettering Cancer Center Support grant P30 CA008748.

Conflicts of interest are listed at the end of this article.

with pathologically proven rectal adenocarcinoma between May 2012 and May 2014. Among them, 31 patients (mean age, 65 years [range, 32–84 years]; 22 men [mean age, 64 years; range, 52–84 years]; and nine women [mean age, 67 years; range, 32–83 years]; $P = .5$) satisfied the following inclusion criteria: *(a)* histologically confirmed rectal adenocarcinoma; *(b)* locally advanced rectal cancer (stage T3–T4) at pre-CRT MR imaging; *(c)* pre- and post-CRT MR imaging, including DWI sequences with multiple *b* values; *(d)* neoadjuvant CRT; and *(e)* surgical resection. Ninety-two patients were excluded for the following reasons: poor image quality ($n = 9$), lack of DWI sequences with multiple *b* values ($n = 70$), or stage T1 or T2 disease ($n = 13$).

The median time intervals were as follows: 124 days (range, 65–254 days) between pre-CRT MR imaging and surgery, 88 days (range, 56–210 days) between pre- and post-CRT MR imaging, and 36 days (range, 1–58 days) between post-CRT MR imaging and surgery. The median time interval between the completion of CRT and surgery was 66 days (range, 53–81 days).

Preoperative CRT

All patients underwent three-dimensional conformal treatment planning by using computed tomographic (CT) simulation (PQ 2000 CT Simulator; Marconi Medical Systems, Cleveland, Ohio). Preoperative radiation therapy at a dose of 45 Gy in 25 fractions was delivered to the pelvis in 22 patients (22 of 31 patients, 71%). Nine patients (nine of 31, 29%) received a boost of 5.4 Gy in three fractions and in a limited volume. Chemotherapy was performed concomitantly with radiation therapy by using capecitabine (Xeloda, Roche, Basel, Switzerland; 800 mg/m^2 twice daily during radiation therapy days) in 21 patients (21 of 31, 68%) or oxaliplatin (Eloxatin, Sanofi-Aventis, Paris, France; 85 mg/m^2 on day 1) plus leucovorin (Elvorin, Sanofi-Aventis; 200 mg/m^2 on days 1 and 2) and fluorouracil (Sanofi-Aventis; 400-mg/m^2 bolus followed by a 600-mg/m^2 infusion over 22 hours on days 1 and 2) in 10 patients (10 of 31, 32%).

Table 1

DWI and T2-weighted Pulse Sequence Parameters

Parameter	IVIM Sequence	T2-weighted Sequence
Acquisition plane	Axial, angled perpendicular to tumor	Axial, angled perpendicular to tumor
Repetition time (msec)/echo time (msec)	3925/minimum	3000/102
b values (sec/mm^2)	0, 10, 15, 20, 25, 30, 35, 40, 45, 50, 55, 60, 65, 70, 75, 80, 85, 90, 95, 100, 105, 110, 115, 120, 125, 130, 135, 140, 145, 150, 155, 160, 800, 1500	…
Echo train length	…	22
Section thickness (mm)	6	3
Intersection gap (mm)	0	0
Imaging time (min)	5	5
Acquisition matrix	126 × 256	256 × 256
Parallel imaging factor	2	…
Echo-planar imaging factor	64	…
No. of signals acquired	1 below *b* values of 800 sec/mm^2 and 8 for *b* values of 800 sec/mm^2 and higher	3

MR Imaging Technique

Pre- and post-CRT MR imaging was performed with a 1.5-T imaging unit (Signa EXCITE HD; GE Medical Systems, Milwaukee, Wis) by using an eight-element pelvic phased-array surface coil. The examination protocol did not change over the 2-year study period. Pulse sequences and pulse sequence parameters are detailed in Table 1 and are briefly described as follows.

T2-weighted imaging was performed in the axial oblique, coronal, and sagittal planes. The axial oblique planes were angled perpendicularly along the long axis of the tumor by using the sagittal plane, as described by Brown et al (25).

The DWI pulse sequence was performed in the same orientation as axial oblique T2-weighted imaging by using respiratory-triggered fat-saturated spin-echo echo-planar imaging. The following 34 *b* values were used: 0, 10, 15, 20, 25, 30, 35, 40, 45, 50, 55, 60, 65, 70, 75, 80, 85, 90, 95, 100, 105, 110, 115, 120, 125, 130, 135, 140, 145, 150, 155, 160, 800, and 1500 sec/mm^2. The distribution of *b* values was chosen to cover both the initial pseudodiffusion decay (≤200 sec/mm^2) and the molecular diffusion decay (>200 sec/mm^2). We used a large number of lower *b* values for more accurate calculation of the fast diffusion coefficient *(D*)*.

The total acquisition time was approximately 30 minutes, including the IVIM sequence, which lasted 5 minutes. Patients did not undergo bowel preparation or receive antispasmodic medication or intravenous contrast material. Our routine protocol did not include rectal distension. However, if the tumor was too small to identify on the sagittal T2-weighted images after CRT, a small amount of gel (Lumirem; Guerbet, Villepinte, France) was instilled into the rectum prior to further image acquisition.

IVIM analysis.—Diffusivity values were set as follows: 1, diffusion coefficient of slow or non–perfusion-related diffusion, which represents true molecular diffusion, termed *D* (given in units of $\times 10^{-3}$ mm^2/sec); 2, diffusion coefficient of fast or perfusion-related diffusion, termed *D** (given in units of $\times 10^{-3}$ mm^2/sec); 3, perfusion-related diffusion fraction, which represents fractional volume occupied in the voxel by flowing spins, termed *f* (given as a percentage); and 4, monoexponential ADC, which was noted as ADC (and given in units of $\times 10^{-3}$ mm^2/sec).

These diffusivity values were calculated by using the IVIM model equation described by Le Bihan (26) and Le Bihan et al (27):

$$\frac{Sb}{S0} = (1-f)x\exp^{(-bD)} + fx\exp^{(-bD*)},$$

where S is the mean signal intensity, Sb is the signal intensity in the pixel with diffusion gradient b, and $S0$ is the signal intensity in the pixel without diffusion gradient.

The calculation was performed by using Olea Medical Software (Olea Medical, La Ciotat, France) that provided the D, D^*, f, and ADC metrics mapped on a pixel-by-pixel basis (Fig 1). The mean processing time to automatically generate the IVIM parameters was 5 minutes 37 seconds.

Whole-tumor volume analysis.—For each patient, two readers who were blinded to the histopathology results (fellowship-trained radiologists with 5 years [S.N.] and 10 years [H.A.V.] of experience in oncologic body imaging) independently determined the whole-tumor volume before and after CRT by manually tracing the outer edge of the lesion on each D image with reference to the T2-weighted image (fused D and T2-weighted images). Whole-tumor volume was automatically calculated by summing each of the cross-sectional volumes (multiplying cross-sectional area by section thickness) with the same dedicated software (Olea Medical Software; Olea Medical).

The software automatically copied and pasted whole-tumor volumes onto all other IVIM (D^*, f) and ADC images (Fig 1). When no residual tumor was seen on the post-CRT images obtained with the DWI pulse sequence (three cases), tracings were placed on the rectal wall at the site of prior tumor. Each of the ADC, D, D^*, and f values per pixel from the whole-tumor volume were imported into R version 2.15.2 (R Foundation for Statistical Computing, Vienna, Austria). The minimum, 10th, 25th, 50th, 75th, and 90th percentile pixel values and the maximal pixel values were generated, and the skewness and kurtosis of the histogram were recorded. Skewness and kurtosis reflect the shape of a histogram and were used to measure the asymmetry of the ADC, D^*, D, and f value distribution around the mean. Skewness is positive if most of the data are concentrated on the left of the histogram and negative if most of the data are concentrated on the right. Kurtosis represented the concentration of values around the mean and reflected the peak of the distribution. In a normal distribution, skewness is 0, and kurtosis is 3.

Percentage changes in ADC ($ADC\%$ in the following equation) and D ($D\%$ in the following equation) were calculated as follows:

$$ADC\% = \frac{(ADCpos - ADCpre)}{ADCpre} \times 100$$

and

$$D\% = \frac{(Dpost - Dpre)}{Dpre} \times 100,$$

where $ADCpost$ represents post-CRT ADC values, $ADCpre$ represents pre-CRT ADC values, $Dpost$ represents post-CRT D values, and $Dpre$ represents pre-CRT D values.

Single-section ROI analysis.—For the single-section ROI analysis, the same two readers independently drew a single freehand ROI that contained the largest available tumor area on a single representative section. Pre- and post-CRT D and ADC histogram values were obtained from the single-section ROIs by using the same method detailed earlier. Since the initial f and D^* data obtained from the whole-tumor volume analysis were not useful for the subsequent analysis, these IVIM measures were not reported in the single-section ROI methods for the sake of simplicity.

Surgical Resection

One colorectal surgeon (P.R., with 18 years of experience) performed all surgical resections, consisting of total mesorectal excision, at a minimum. The mesorectum was transected, along with an adequate distal margin according to the tumor level. All surgical procedures are summarized in Table 2.

Histopathologic Examination

Each specimen was opened along the anterior border proximal to the tumor-containing segment and was fixed with total immersion into buffered formalin for 48 hours. The longest dimension was measured by using a metric ruler. Embedded histopathologic slides were evaluated by one pathologist (F.B., with 17 years of experience). Pathologic tumor staging was performed according to the TNM system (28). Evaluation of the CRT response involved the tumor regression grade, or TRG, system proposed by Dworak et al (29), from no tumor regression (grade 0) to a complete response (grade 4). Patients with TRG grades 0–2 are considered to have a poor pathologic response, whereas patients with TRG grades 3–4 are considered to have a good pathologic response.

Statistical Analysis

Interobserver agreement for whole-tumor volume and single-section measurements was analyzed by calculating the interclass correlation coefficient and was interpreted as follows: 0.00–0.20, poor correlation; 0.21–0.40, fair correlation; 0.41–0.60, moderate correlation; 0.61–0.80, good correlation; and 0.81–1.00, excellent correlation. Since the interobserver agreement for the whole-tumor volume was excellent, only the first reader results were used for further analysis. The differences in variance between ADC and IVIM histogram metrics were tested with the Pitman test for paired data. Analysis of variance for repeated measures with Holm-Sidak correction for multiple comparisons was used to compare pre- and post-CRT ADC and IVIM measures. We used t tests with Holm-Sidak correction to compare ADC and IVIM diffusion metrics and the variations between them for good and poor responders to CRT. Receiver operating characteristic (ROC) curves were generated to evaluate the diagnostic performance of ADC and IVIM histogram metrics and median values for the assessment of histopathologic response. The optimal threshold was chosen according to the Youden index. Owing to the small size of the data set and because we wanted to improve the robustness of our results,

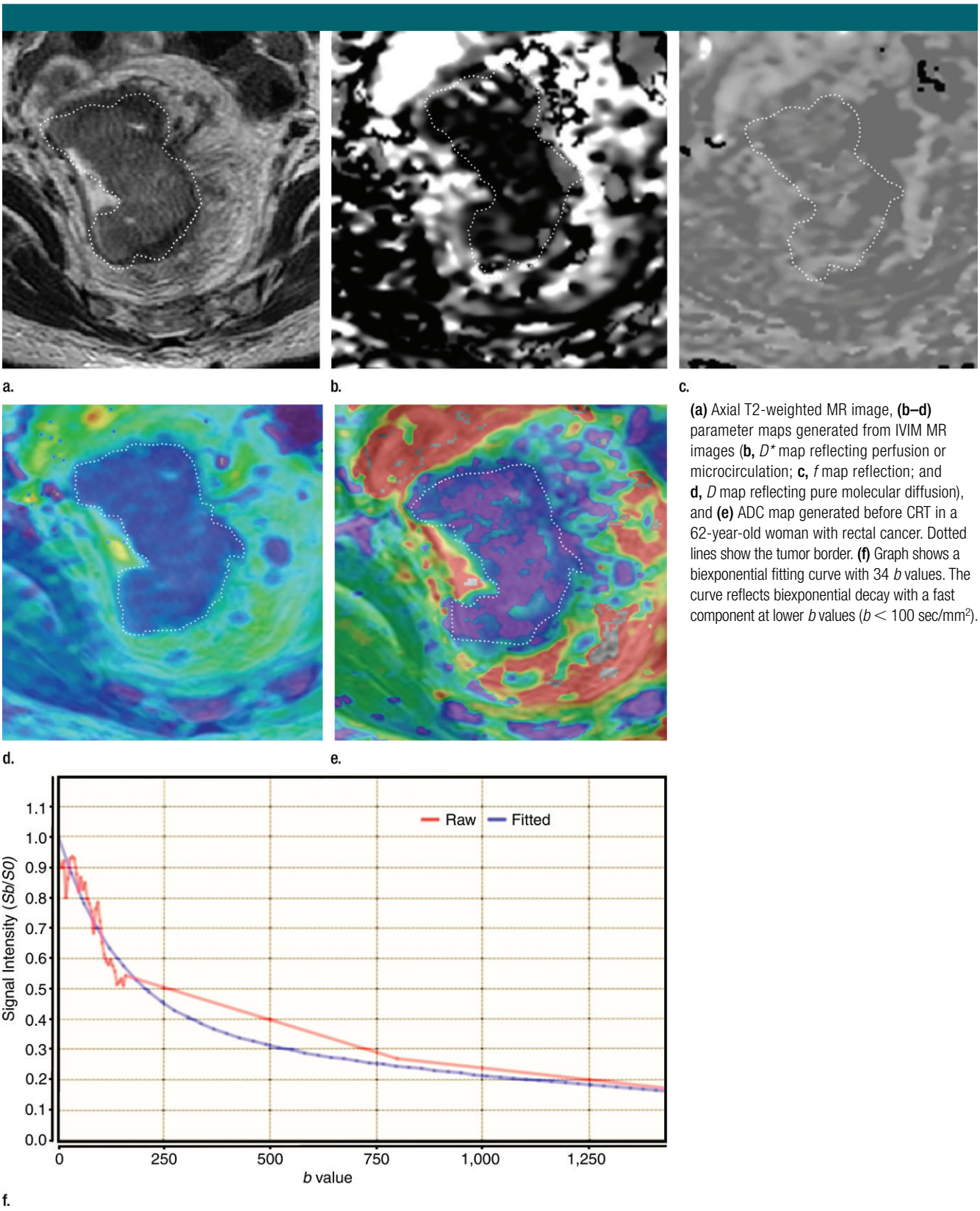

(a) Axial T2-weighted MR image, **(b–d)** parameter maps generated from IVIM MR images (**b,** D^* map reflecting perfusion or microcirculation; **c,** f map reflection; and **d,** D map reflecting pure molecular diffusion), and **(e)** ADC map generated before CRT in a 62-year-old woman with rectal cancer. Dotted lines show the tumor border. **(f)** Graph shows a biexponential fitting curve with 34 b values. The curve reflects biexponential decay with a fast component at lower b values ($b < 100$ sec/mm^2).

Table 2

Baseline and Demographic Data in 31 Patients

Characteristic	Value
Patient sex	
No. of men	22 (71)
No. of women	9 (29)
Age (y)	
All patients	65 [32–84]
Men	64 [52–84]
Women	67 [32–83]
Distance of the primary tumor from the anus	
0–5.0 cm	10 (32)
5.1–10.0 cm	18 (58)
10.1–15.0 cm	3 (10)
Surgery performed	
Low anterior resection	4 (13)
Proctectomy with coloanal anastomosis	3 (10)
Proctectomy with colorectal anastomosis	24 (77)
Posttreatment pathologic T (ypT) classification	
YpT0	5 (16)
YpT1-YpT2	12 (39)
YpT3	12 (39)
YpT4	2 (6)
Tumoral regression grade*	
Grade 0	2 (6)
Grade 1	5 (16)
Grade 2	7 (22)
Grade 3	12 (39)
Grade 4	5 (16)
Circumferential resection margin at histopathologic examination	
≤1 mm	0 (0)
>1 mm	31 (100)

Note.—Continuous data are expressed as means, with ranges in brackets. Categorical data are expressed as numbers of patients, with percentages in parentheses.

* According to Dworak et al (29).

Table 3

Diagnostic Performance of Post-CRT *D* and ADC Histogram Metrics Obtained by Using Whole-Tumor Volume Analysis for the Detection of Good Response to CRT

Post-CRT Metric	Minimum	10th Percentile	25th Percentile	50th Percentile	75th Percentile	90th Percentile	Maximum
D							
Area under the ROC curve (AUC)	0.77	0.97	0.98	0.98	0.98	0.96	0.6
Confidence interval	0.6, 0.9	0.8, 1	0.8, 1	0.8, 1	0.9, 1	0.8, 1	0.4, 0.7
Sensitivity (%)	94	94	94	94	94	100	71
Specificity (%)	57	92	100	100	92	77	57
P value	.0012	.0001	.0001	.0001	.0001	.0001	.3
Cutoff calculated	0.1	0.7	0.85	1	1.1	1.1	1.7
ADC							
AUC	0.8	0.88	0.90	0.86	0.85	0.87	0.6
Confidence interval	0.6, 0.9	0.7, 0.9	0. 8, 1	0.7, 0.9	0.6, 0.9	0.7, 0.9	0.4, 0.8
Sensitivity (%)	94	76	82	82	88	88	58
Specificity (%)	64	85	92	85	78	85	78
P value	.001	.0001	.0001	.0001	.0001	.0001	.1
Cutoff calculated	0.433	0.45	1.1	1.3	1.3	1.5	2.3

the discriminative ability of the model was estimated by using a leave-one-out approach. For each data set with one removed value, the optimal threshold and the accuracy of these values were calculated, and the removed value was compared with the prediction to estimate the predicted power of the model. ROC curves of histogram metrics for the discrimination between good and poor responders were compared with each other to assess potential differences. A *P* value of less than .05 was considered to indicate a statistically significant difference. Statistical analyses were performed by using GraphPad software (Prism 6; GraphPad Software, La Jolla, Calif) and R version 3.1.1 (R Foundation).

Results

Clinical Characteristics

Of the 31 patients, five patients (16%) had complete response to CRT, and 17 patients (55%) had good response to CRT (Table 2).

Whole-Tumor Post-CRT ADC and IVIM Histogram Metrics over Median Values

Aside from the upper and lower extreme values, the post-CRT histogram metrics were significantly associated with tumor response to CRT (Table 3; Tables E1–E6 [online]). No difference in variance was found between the minimum, 10th, 25th, 75th, and 90th percentiles of *D* over the median *D* value (P = .12, .31, .63, .6, and .5, respectively). Likewise, no difference in variance was found between the minimum, 10th, 25th, 75th, and 90th percentiles of ADC over the median ADC value (P = .06, .28, .97, .75, and .51, respectively). Maximum histogram metrics of *D* and ADC showed wider variance compared with the median value ($P < .0001$ and $P = .003$, respectively).

Post-CRT *D* and ADC histogram metrics (10th, 25th, 50th, 75th, and 90th percentiles) had similar AUC values and were equivalent to each other for the detection of good responders to CRT (Table 3). Minimum and maximum *D* histogram metrics had significantly lower AUCs when compared with 10th, 25th, 50th, 75th, and 90th histogram metrics ($P \leq .02$ and $P < .01$, respectively). Maximum ADC histogram metrics had significantly lower AUCs when compared with 25th, 50th, 75th, and 90th percentiles ($P < .01$).

Since histogram metrics were not significantly better than median values for the assessment of treatment response and for the discrimination between good and poor responders to CRT, all subsequent analysis was restricted to median values. Complete analysis is shown in Tables 1–3, Tables E1–E8 (online), and Figures E1 and E2 (online).

Whole-Tumor Pre- and Post-CRT Median ADC and IVIM Values for Response Assessment

Median *D* and ADC values increased significantly between pre- and post-CRT MR imaging studies ($P < .0001$ and $P = .0009$, respectively) and were significantly higher in good versus poor responders to CRT ($P < .0001$ and $P = .002$, respectively; Tables E2, E3 [online]). The median *D* was lower than the median ADC before and after CRT ($P \leq .0001$ and $P \leq .01$, respectively). The relative change in these same parameters was significantly greater in the good responders compared with the poor responders ($P < .0001$ and $P = .004$, respectively; Table E4 [online]; Figs E1, E2 [online]). Prior to CRT, none of the median *f*, *D**, *D*, and ADC values were significantly different between good and poor responders (Table E3 [online]).

Changes in median *f* and *D** values before and after CRT were not associated with the degree of tumor response (Tables E2, E3 [online]).

Median *D* values demonstrated a tendency toward higher AUCs (AUC of 0.98) than the median ADC values (AUC of 0.86) for the assessment of treatment response, but this difference did not reach statistical significance ($P = .07$; Table 3). However, when median *D* values were used, leave-one-out cross-validation showed that predictions were correct in 28 of the 31 patients (90%) in their initial groups. On the other hand, when median ADC values were used, leave-one-out cross-validation was used to accurately assess CRT response in only 20 of the 31 patients (64%).

Whole-Tumor Volume Analysis over Single-Section ROI Analysis

The analysis of single-section ROI and whole-tumor volume data produced similar results regarding changes in diffusion measures after CRT and discrimination between good versus poor responders to CRT. Pairwise comparison of ROC curves for *D* and ADC histogram metrics computed by using whole-tumor volumes and single-section ROIs demonstrated no statistically significant differences. Median *D* and ADC values obtained from single-section ROIs increased significantly after CRT (*D* for reader 1, $P = .01$; *D* for reader 2, $P = .002$; ADC for reader 1, $P = .0006$; ADC for reader 2, $P = .0002$) and were significantly higher in good versus poor responders to CRT (*D* for reader 1, $P = .003$; *D* for reader 2, $P = .004$; ADC for reader 1, $P = .02$; ADC for reader 2, $P = .02$; Tables E5, E6 [online]). For response assessment to CRT, the AUC of the median single-section ROI *D* after CRT was higher than the median single-section ROI ADC (Table E1 [online]) for both readers (reader 1, 0.84 vs 0.77, respectively; reader 2, 0.79 vs 0.74, respectively), although the difference did not reach statistical significance.

Whole-tumor volume analysis was found to have excellent interobserver agreement for pre- and post-CRT median *D* and ADC values (range, 0.91–0.95). The interobserver agreement was only moderate when median single-section ROI analysis was used (range, 0.50–0.63). Interclass correlation coefficients between the two readers are provided in Tables E7 and E8 (online).

Discussion

We found that IVIM-derived diffusion coefficient *D* and DWI-derived ADC are useful for the assessment of tumor response to CRT, in that they increased significantly after CRT and were significantly higher in good versus poor responders. We found histogram metrics to be equivalent to the median values, which suggests that it is sufficient and acceptable to use median values in everyday clinical practice. Finally, the whole-tumor volume analysis led to more reproducible results when compared with single-section ROI analysis.

This association between tumor response and ADC values has been reported previously (18,24,30,31). Our data demonstrated that the ADC values before and after CRT were significantly higher than their *D* values, supporting the notion that perfusion contributes to the ADC in rectal cancer, as observed previously in other tumors and organs (32–34). Microcirculation or perfusion effects can be distinguished from the true tissue diffusion by means of sufficient *b* value sampling and a biexponential curve fit analysis by using IVIM imaging (26,27). With the use of the IVIM method, both true molecular diffusion and water molecule motion in the capillary network can be estimated with a single diffusion imaging acquisition.

We found that IVIM-derived *f* and *D** values did not significantly change before and after CRT and were not useful for the assessment of tumor response to CRT. Our results are concordant with those of prior studies that were focused on the liver (32–34). The limited value of *D** was previously explained by its high uncertainty and poor reproducibility (33,35–37). Similarly, in our study, the interclass correlation coefficients for *D** ranged from 0.23 to 0.82.

Although we did not demonstrate the added value of *f*, this result should be interpreted with caution. The *f* value is affected by the T2 contributions of both perfusion and pure molecular diffusion compartments (36,38). The biexponential IVIM model indicates that *f* is defined as the signal intensity ratio of blood capillaries and tumor tissues. In this analysis, all relaxation effects are ignored. This is acceptable as long as the relaxation times of the tumor and the capillary blood are similar. However, at times, the T2 contributions of the tumor and blood capillaries can be substantially different. It is well known that after CRT, T2 of the tumor tends to increase (38), which could artificially lower calculated *f* values. The underestimation of *f* increases both with the longer echo times and with the increased differences in T2 between the capillary blood and tissue.

To our knowledge, prior studies in which investigators evaluated the value of DWI in rectal cancer relied on the selected ROIs that were placed inside a tumor on a representative section. While it is a simple and practical approach, it is potentially limited by the inaccuracies introduced by the variations in ROI size and positioning (15,22–24). In comparison to the single-section ROI method, whole-tumor

volume analysis involves sampling of the entire tumor, which may minimize sampling bias. Furthermore, whole-tumor volume analysis may better capture the inherent intratumoral heterogeneity and improve its assessment (39). As described previously (39,40), our results indicate that whole-tumor volume analysis of diffusion metrics yields more reproducible data than does single-section ROI analysis. We also evaluated the added value of histogram metrics over the median values for the assessment of tumor response to CRT. Histograms have been applied to brain imaging and, more recently, to the evaluation of ovarian, prostate, and endometrial cancers (41). We found that except for extreme values, histogram metrics for *D* and ADC obtained from the whole-tumor volume were equivalent to the median values for the assessment of post-CRT treatment response and for the discrimination between good versus poor responders to CRT. Thus, our results suggest that in the routine clinical setting, the use of median ADC and IVIM values obtained by using whole-tumor volume analysis is the preferred approach for the assessment of tumor response to CRT in rectal cancer. Furthermore, the minimum and maximum diffusion values should be avoided.

Our study has several limitations. To begin with, the sample size was relatively small. Since some imaging studies were performed at outside institutions, many patients were excluded from our study cohort because of the lack of pulse sequences with multiple *b* values used to acquire either pre-CRT or post-CRT MR images. Second, we did not compare our findings with the tumor perfusion data from the dynamic contrast material–enhanced acquisitions. Third, the perfusion fraction *f* values were not T2 corrected, as recommend by some authors (36,38) and thus could have been influenced by the T2 relaxation times of blood and tissues. Fourth, when using volumetric analysis, there is a possibility that misregistration artifacts could have been included for extreme ADC, *D*, *D**, and *f* values. It can be presumed that the 10th or 90th percentile values obtained from ADC histograms are less affected by these artifacts and therefore would be more reliable for histogram analysis than the minimum or maximum ADC values. Finally, the evaluation was based on the scoring system of Dworak et al (29) but only had a final binary outcome assessment of good or poor responders. Use of an intermediate grade might improve accuracy (42,43). Given the small sample of this preliminary study, this kind of analysis was not possible.

In summary, our preliminary results indicate that median ADC and *D* values are useful for the assessment of tumor response to CRT in rectal cancer and for the discrimination between good and poor responders. Larger, preferably prospective studies are needed to further delineate the value of *D* as a noninvasive imaging biomarker in rectal cancer. Histogram analysis does not yield better results than median values and may not be necessary in routine clinical practice. Whole-tumor volume is preferred over single-section ROI analysis because of its superior interobserver agreement and the potential to better capture the intratumoral heterogeneity.

Acknowledgments: The authors thank Guillaume Lafarge, MD, Corrado Rovani, MD, and Raphael Tetreau, MD, for their kind assistance with this project.

Disclosures of Conflicts of Interest: S.N. disclosed no relevant relationships. **A.V.** disclosed no relevant relationships. **Y.L.** disclosed no relevant relationships. **R.S.** disclosed no relevant relationships. **R.K.G.D.** disclosed no relevant relationships. **F.B.** disclosed no relevant relationships. **D.A.** disclosed no relevant relationships. **E.A.** disclosed no relevant relationships. **N.M.** disclosed no relevant relationships. **M.A.P.** disclosed no relevant relationships. **P.R.** disclosed no relevant relationships. **B.G.** disclosed no relevant relationships.

References

1. Bhangu A, Ali SM, Cunningham D, Brown G, Tekkis P. Comparison of long-term survival outcome of operative vs nonoperative management of recurrent rectal cancer. Colorectal Dis 2013;15(2):156–163.
2. Habr-Gama A, de Souza PM, Ribeiro U Jr, et al. Low rectal cancer: impact of radiation and chemotherapy on surgical treatment. Dis Colon Rectum 1998;41(9):1087–1096.
3. Habr-Gama A, Perez RO, Proscurshim I, et al. Absence of lymph nodes in the resected specimen after radical surgery for distal rectal cancer and neoadjuvant chemoradiation therapy: what does it mean? Dis Colon Rectum 2008;51(3):277–283.
4. Habr-Gama A, Perez RO, São Julião GP, Proscurshim I, Nahas SC, Gama-Rodrigues J. Factors affecting management decisions in rectal cancer in clinical practice: results from a national survey. Tech Coloproctol 2011;15(1):45–51.
5. Maas M, Beets-Tan RG, Lambregts DM, et al. Wait-and-see policy for clinical complete responders after chemoradiation for rectal cancer. J Clin Oncol 2011;29(35):4633–4640.
6. Kosinski L, Habr-Gama A, Ludwig K, Perez R. Shifting concepts in rectal cancer management: a review of contemporary primary rectal cancer treatment strategies. CA Cancer J Clin 2012;62(3):173–202.
7. Habr-Gama A, Sabbaga J, Gama-Rodrigues J, et al. Watch and wait approach following extended neoadjuvant chemoradiation for distal rectal cancer: are we getting closer to anal cancer management? Dis Colon Rectum 2013;56(10):1109–1117.
8. Habr-Gama A, Gama-Rodrigues J, São Julião GP, et al. Local recurrence after complete clinical response and watch and wait in rectal cancer after neoadjuvant chemoradiation: impact of salvage therapy on local disease control. Int J Radiat Oncol Biol Phys 2014;88(4):822–828.
9. Hicks RJ, Ware RE, Lau EW. PET/CT: will it change the way that we use CT in cancer imaging? Cancer Imaging 2006;6:S52–S62.
10. Lambrecht M, Deroose C, Roels S, et al. The use of FDG-PET/CT and diffusion-weighted magnetic resonance imaging for response prediction before, during and after preoperative chemoradiotherapy for rectal cancer. Acta Oncol 2010;49(7):956–963.
11. Allen SD, Padhani AR, Dzik-Jurasz AS, Glynne-Jones R. Rectal carcinoma: MRI with histologic correlation before and after chemoradiation therapy. AJR Am J Roentgenol 2007;188(2):442–451.
12. Al-Sukhni E, Milot L, Fruitman M, et al. Diagnostic accuracy of MRI for assessment of T category, lymph node metastases, and circumferential resection margin involvement in patients with rectal cancer: a systematic review and meta-analysis. Ann Surg Oncol 2012;19(7):2212–2223.
13. Heald RJ, O'Neill BD, Moran B, et al. MRI in predicting curative resection of rectal can-

cer: new dilemma in multidisciplinary team management. BMJ 2006;333(7572):808.

14. Beets-Tan RG, Beets GL, Vliegen RF, et al. Accuracy of magnetic resonance imaging in prediction of tumour-free resection margin in rectal cancer surgery. Lancet 2001;357 (9255):497–504.

15. Lambregts DM, Vandecaveye V, Barbaro B, et al. Diffusion-weighted MRI for selection of complete responders after chemoradiation for locally advanced rectal cancer: a multicenter study. Ann Surg Oncol 2011;18(8): 2224–2231.

16. Jang KM, Kim SH, Choi D, Lee SJ, Park MJ, Min K. Pathological correlation with diffusion restriction on diffusion-weighted imaging in patients with pathological complete response after neoadjuvant chemoradiation therapy for locally advanced rectal cancer: preliminary results. Br J Radiol 2012; 85(1017):e566–e572.

17. Song I, Kim SH, Lee SJ, Choi JY, Kim MJ, Rhim H. Value of diffusion-weighted imaging in the detection of viable tumour after neoadjuvant chemoradiation therapy in patients with locally advanced rectal cancer: comparison with T2 weighted and PET/CT imaging. Br J Radiol 2012;85(1013):577–586.

18. Genovesi D, Filippone A, Ausili Cèfaro G, et al. Diffusion-weighted magnetic resonance for prediction of response after neoadjuvant chemoradiation therapy for locally advanced rectal cancer: preliminary results of a monoinstitutional prospective study. Eur J Surg Oncol 2013;39(10):1071–1078.

19. Curvo-Semedo L, Lambregts DM, Maas M, et al. Rectal cancer: assessment of complete response to preoperative combined radiation therapy with chemotherapy—conventional MR volumetry versus diffusion-weighted MR imaging. Radiology 2011;260(3):734–743.

20. Lambregts DM, Rao SX, Sassen S, et al. MRI and diffusion-weighted MRI volumetry for identification of complete tumor responders after preoperative chemoradiotherapy in patients with rectal cancer: a bi-institutional validation study. Ann Surg 2015;262(6): 1034–1039.

21. Barbaro B, Vitale R, Valentini V, et al. Diffusion-weighted magnetic resonance imaging in monitoring rectal cancer response to neoadjuvant chemoradiotherapy. Int J Radiat Oncol Biol Phys 2012;83(2):594–599.

22. Kim SH, Lee JM, Hong SH, et al. Locally advanced rectal cancer: added value of diffusion-weighted MR imaging in the evaluation of tumor response to neoadjuvant chemo- and radiation therapy. Radiology 2009;253(1): 116–125.

23. Park MJ, Kim SH, Lee SJ, Jang KM, Rhim H. Locally advanced rectal cancer: added value of diffusion-weighted MR imaging for predicting tumor clearance of the mesorectal fascia after neoadjuvant chemotherapy and radiation therapy. Radiology 2011;260(3): 771–780.

24. Kim SH, Lee JY, Lee JM, Han JK, Choi BI. Apparent diffusion coefficient for evaluating tumour response to neoadjuvant chemoradiation therapy for locally advanced rectal cancer. Eur Radiol 2011;21(5):987–995.

25. Brown G, Richards CJ, Newcombe RG, et al. Rectal carcinoma: thin-section MR imaging for staging in 28 patients. Radiology 1999;211(1):215–222.

26. Le Bihan D. Intravoxel incoherent motion perfusion MR imaging: a wake-up call. Radiology 2008;249(3):748–752.

27. Le Bihan D, Breton E, Lallemand D, Aubin ML, Vignaud J, Laval-Jeantet M. Separation of diffusion and perfusion in intravoxel incoherent motion MR imaging. Radiology 1988; 168(2):497–505.

28. Edge SB, Compton CC. The American Joint Committee on Cancer: the 7th edition of the AJCC cancer staging manual and the future of TNM. Ann Surg Oncol 2010;17(6):1471–1474.

29. Dworak O, Keilholz L, Hoffmann A. Pathological features of rectal cancer after preoperative radiochemotherapy. Int J Colorectal Dis 1997;12(1):19–23.

30. Jung SH, Heo SH, Kim JW, et al. Predicting response to neoadjuvant chemoradiation therapy in locally advanced rectal cancer: diffusion-weighted 3 Tesla MR imaging. J Magn Reson Imaging 2012;35(1):110–116.

31. Ha HI, Kim AY, Yu CS, Park SH, Ha HK. Locally advanced rectal cancer: diffusion-weighted MR tumour volumetry and the apparent diffusion coefficient for evaluating complete remission after preoperative chemoradiation therapy. Eur Radiol 2013;23(12):3345–3353.

32. Andreou A, Koh DM, Collins DJ, et al. Measurement reproducibility of perfusion fraction and pseudodiffusion coefficient derived by intravoxel incoherent motion diffusion-weighted MR imaging in normal liver and metastases. Eur Radiol 2013;23(2):428–434.

33. Joo I, Lee JM, Yoon JH, Jang JJ, Han JK, Choi BI. Nonalcoholic fatty liver disease: intravoxel incoherent motion diffusion-weighted MR imaging—an experimental study in a rabbit model. Radiology 2014;270(1):131–140.

34. Woo S, Lee JM, Yoon JH, Joo I, Han JK, Choi BI. Intravoxel incoherent motion diffusion-weighted MR imaging of hepatocellular carcinoma: correlation with enhancement degree and histologic grade. Radiology 2014;270(3):758–767.

35. Dyvorne HA, Galea N, Nevers T, et al. Diffusion-weighted imaging of the liver with multiple b values: effect of diffusion gradient polarity and breathing acquisition on image quality and intravoxel incoherent motion parameters—a pilot study. Radiology 2013;266(3):920–929.

36. Guiu B, Petit JM, Capitan V, et al. Intravoxel incoherent motion diffusion-weighted imaging in nonalcoholic fatty liver disease: a 3.0-T MR study. Radiology 2012;265(1):96–103.

37. Kakite S, Dyvorne H, Besa C, et al. Hepatocellular carcinoma: short-term reproducibility of apparent diffusion coefficient and intravoxel incoherent motion parameters at 3.0T. J Magn Reson Imaging 2015;41(1):149–156.

38. Lemke A, Laun FB, Simon D, Stieltjes B, Schad LR. An in vivo verification of the intravoxel incoherent motion effect in diffusion-weighted imaging of the abdomen. Magn Reson Med 2010;64(6):1580–1585.

39. Goh V, Halligan S, Gharpuray A, Wellsted D, Sundin J, Bartram CI. Quantitative assessment of colorectal cancer tumor vascular parameters by using perfusion CT: influence of tumor region of interest. Radiology 2008;247(3):726–732.

40. Lambregts DM, Beets GL, Maas M, et al. Tumour ADC measurements in rectal cancer: effect of ROI methods on ADC values and interobserver variability. Eur Radiol 2011; 21(12):2567–2574.

41. Donati OF, Mazaheri Y, Afaq A, et al. Prostate cancer aggressiveness: assessment with whole-lesion histogram analysis of the apparent diffusion coefficient. Radiology 2014; 271(1):143–152.

42. Fokas E, Liersch T, Fietkau R, et al. Tumor regression grading after preoperative chemoradiotherapy for locally advanced rectal carcinoma revisited: updated results of the CAO/ARO/AIO-94 trial. J Clin Oncol 2014;32(15):1554–1562.

43. Valentini V, Minsky BD. Tumor regression grading in rectal cancer: is it time to move forward? J Clin Oncol 2014;32(15):1534–1536.